

## Role of PCSK9 in lipid metabolic disorders and ovarian dysfunction in polycystic ovary syndrome

Meijiao Wang<sup>a</sup>, Dan Zhao<sup>a</sup>, Liangzhi Xu<sup>b,c</sup>, Wenjing Guo<sup>a</sup>, Li Nie<sup>a</sup>, Yi Lei<sup>a</sup>, Yun Long<sup>a</sup>, Min Liu<sup>a</sup>, Yichen Wang<sup>a</sup>, Xueqin Zhang<sup>a</sup>, Li Zhang<sup>a</sup>, Hanna Li<sup>a</sup>, Jinhu Zhang<sup>a</sup>, Dongzhi Yuan<sup>a,\*</sup>, Limin Yue<sup>a,\*</sup>

<sup>a</sup> Department of Physiology, West China School of Basic Medical Sciences and Forensic Medicine, Sichuan University, Sichuan, Chengdu, China

<sup>b</sup> Reproductive Endocrinology and Regulation Joint Laboratory, West China Second University Hospital, Sichuan University, Sichuan, Chengdu, China

<sup>c</sup> Department of Obstetrics & Gynecology, West China Second University Hospital, Sichuan, Chengdu, China

### ARTICLE INFO

#### Article history:

Received 29 August 2018

Accepted 9 February 2019

#### Keywords:

Polycystic ovary syndrome

Hypercholesterolemia

Ovarian function

Proprotein convertase subtilisin/kexin type-9

Low-density lipoprotein receptor

Alirocumab

### ABSTRACT

**Background:** Proprotein convertase subtilisin/kexin type 9 (PCSK9) plays a critical role in the cholesterol metabolism by negatively regulating the low-density lipoprotein receptor (LDLR). Lipid metabolic and ovarian disorders are the common clinical manifestation of polycystic ovary syndrome (PCOS). Here, we intended to elucidate the role of PCSK9 in the pathogenesis of PCOS conducted on a human population in case-control design and animal part in an interventional study. **Methods:** We firstly investigated the serum levels of PCSK9 in 46 PCOS patients compared with 49 healthy women as controls, and then developed a PCOS mouse model induced by dehydroepiandrosterone (DHEA) and a high-fat diet (HFD) to determine the role of PCSK9 in abnormal lipid metabolism and ovarian dysfunction of PCOS in four groups ( $n = 40$  per group): control, PCOS mice, PCOS plus alirocumab group, and PCOS plus vehicle group. The expression of PCSK9 in their serum, hepatic and ovarian tissues, serum lipid profiles and hormones were measured. Additionally, mRNA and protein expression levels of LDLR in hepatic and ovarian tissues, ovarian morphology and function were determined. Finally, we used freshly isolated theca-interstitial cells (TICs) and granulosa cells (GCs) from prepubertal normal mice to explore the effect of PCSK9 on LDL uptake of the cells.

**Results:** Serum PCSK9 concentrations were higher in PCOS patients than normal controls ( $P < 0.05$ ). The PCOS model mice exhibited significantly increased serum levels of total cholesterol (TC), LDL-C and high-density lipoprotein-cholesterol (HDL-C;  $P < 0.001$ ,  $P < 0.001$ ,  $P = 0.0004$ , respectively). Moreover, the serum PCSK9 protein level was significantly increased in PCOS mice ( $P = 0.0002$ ), which positively correlated with serum LDL-C ( $r = 0.5279$ ,  $P = 0.0004$ ) and TC ( $r = 0.4151$ ,  $P = 0.035$ ). In both liver and ovary of PCOS mice, PCSK9 mRNA and protein levels were significantly increased ( $P < 0.05$ ), but LDLR levels were significantly decreased ( $P < 0.05$ ). Furthermore, alirocumab inhibiting PCSK9 partly increased in LDLR expression in both liver and ovary in PCOS mice, also ameliorated the lipid metabolic disorders and pathological changes of ovarian morphology and function and serum reproductive hormones but not in the PCOS plus vehicle group. *In vitro* experiment, recombinant PCSK9 decreased LDL uptake in TICs and GCs ( $P < 0.001$ ,  $P = 0.0011$ , respectively), which were partly reversed by alirocumab ( $P < 0.001$ ,  $P = 0.012$ , respectively).

**Conclusion:** Abnormal high expression of PCSK9 in the blood, liver and ovary may be involved in the pathogenesis of PCOS by affecting lipid metabolism and ovarian function, and the inhibition of PCSK9 may partly reverse the pathological changes of PCOS. Our research suggests a possibility of PCSK9 as a new attractive target for diagnosis and treatment of PCOS.

© 2019 Elsevier Inc. All rights reserved.

**Abbreviations:** PCOS, polycystic ovary syndrome; PCSK9, proprotein convertase subtilisin/kexin type-9; LDLR, low-density lipoprotein receptor; BMI, body mass index; ELISA, enzyme-linked immunosorbent assay; DHEA, dehydroepiandrosterone; HFD, high-fat diet; TICs, theca-interstitial cells; GCs, granulosa cells; TC, total cholesterol; HDL-C, high-density lipoprotein-cholesterol; TG, triglycerides; CVD, cardiovascular disease; H&E, hematoxylin and eosin; T, testosterone; E2, estradiol; P4, progesterone; CV, coefficients of variability; FSH, follicle-stimulating hormone; LH, luteinizing hormone; TEM, Transmission electron microscopy; PMSG, pregnant mare's serum gonadotropin; hCG, human chorionic gonadotropin; CL, corpus luteum.

\* Corresponding authors at: Department of Physiology, West China School of Basic Medical Sciences and Forensic Medicine, Sichuan University, No. 17 Section 3 Renmin South Road, Chengdu 610041, China.

E-mail addresses: [yuandongzhi@scu.edu.cn](mailto:yuandongzhi@scu.edu.cn) (D. Yuan), [yuelimin@scu.edu.cn](mailto:yuelimin@scu.edu.cn) (L. Yue).

### 1. Introduction

Polycystic ovary syndrome (PCOS) is one of the most common endocrinopathies. It is characterized by hyperandrogenism, ovarian dysfunction, polycystic ovarian morphology [1–3] and metabolic disorders that include insulin resistance and dyslipidemia [4], affecting approximately 5% to 10% of women of reproductive age [2]. Although the disease shows a high degree of heterogeneity and many individual differences, dyslipidemia is one of its most common characteristics, affecting nearly 70% of PCOS patients in the United States [4] and Brazil [5], 36% in the Mediterranean area [6], 48.3% in China [7] and

manifesting elevated low-density lipoprotein (LDL), triglycerides (TG)s, and decreased high-density lipoprotein (HDL) levels [8]. Many PCOS patients are also obese and have atherogenic dyslipidemia, associated with higher rates of cardiovascular disease (CVD) risk [9].

Proprotein convertase subtilisin/kexin type 9 (PCSK9) is a lipid metabolic regulator, found in 2003, the ninth member of the proprotein convertase family [10]. PCSK9 is a protein convertase that post-translationally promotes the degradation of the low-density lipoprotein receptor (LDLR) to the lysosomes in hepatocytes and has been shown to modulate the level of LDLR protein, indicating that it is a critical regulator of cholesterol homeostasis [11]. Gain-of-function mutations of the PCSK9 gene may increase circulating LDL-cholesterol (LDL-C), thus leading to hypercholesterolemia, whereas loss-of-function mutations in PCSK9 are associated with reduced LDL-C, cause hypocholesterolemia [12]. Therefore, PCSK9 has become an important therapeutic target in treatment of hyperlipidemia and CVD [13].

There is a close relationship between lipid metabolism and ovarian function, and research in this area has received increasing attention in recent years. Previous study has shown that follicular fluid contains various lipid forms almost the same as sera [14]. Cholesterol, as a precursor of steroid hormones and material for cell proliferation, is pivotal for ovarian endocrine and follicular development and maturation [15]. Current evidence has suggested that plasma lipoproteins are the major source of cholesterol for steroid production in the ovaries [16]. LDL-C in circulating blood can be directly taken up by the theca-interstitial cells (TICs) and granulosa cells (GCs), and can also enter the follicular fluid through the blood-follicle barrier, where the uptake by the oocytes is beneficial [17]. Uptake of LDL-C by follicular cells can be LDLR-mediated [18]. Thus, it is not surprising that steroidogenic tissues and cell types have evolved multiple pathways to ensure adequate provision of this crucial lipid, including its synthesis, storage as cholesteryl esters and import from lipoproteins [19]. It is not difficult to imagine that abnormalities in whole-body lipid metabolism can directly or indirectly affect the growth and function of follicles by affecting the local microenvironment of follicular fluid. Any factors affecting the uptake of LDL-C by follicular cells and the local microenvironment of follicular fluid will inevitably affect the growth of follicles and their function. Substantial quantities of cholesterol must be either transported into follicular cells and ultimately oocytes, or synthesized locally by the TICs and GCs. However, excessive lipids are the major risk factors for dyslipidemia of PCOS. We thus speculated that PCSK9 may be involved in PCOS. However, the role of PCSK9 in lipid metabolism and follicular development in the pathogenesis of PCOS remains unknown.

In the present research, we collected serum samples of PCOS patients to check their PCSK9 and compare them with those of normal women. Furthermore, we developed a PCOS mouse model induced by dehydroepiandrosterone (DHEA) and a high-fat diet (HFD) to determine the role of PCSK9 and its contribution to the abnormal lipid metabolism and ovarian dysfunction of PCOS. Moreover, we also used alirocumab, a monoclonal antibody for PCSK9 inhibition, to study whether it can reverse the pathological changes of PCOS in the model mice.

## 2. Materials and Methods

### 2.1. Ethics

All human part participants gave their informed consent, and the study was approved by the Ethics Committee of the Sichuan University.

All animal studies were conducted with the approval from the Animal Use and Care Committee of Sichuan University.

### 2.2. Human Case-Control Study

A total of 95 Chinese Han women of similar age were enrolled from the Outpatient Clinic of Reproductive Endocrinology, West China Second University Hospital, Sichuan University. Included were 46 PCOS

patients and 49 healthy women as controls, with the definition of PCOS based on the revised 2003 Rotterdam diagnostic criteria [2]: oligo-anovulation; biochemical and/or clinical hyperandrogenism; polycystic ovaries by ultrasonic examination, with exclusion of other etiologies such as congenital adrenal hyperplasia, androgen-secreting carcinomas and Cushing's syndrome. Control subjects had regular menstrual cycles, normal androgen levels, no evidence of hyperandrogenism and normal ovarian morphology as determined by ultrasound.

The blood samples for the PCSK9 ELISA assay were obtained at random from clinical patients, and samples for other tests were obtained in the morning after being fasted for 12 h on the third to fifth days of the menstrual cycle from regularly menstruating women, placed on ice immediately and centrifuged at 3500 rpm for 15 min at 4 °C within 2 h. Serum samples were stored in 200 mL aliquots at –80 °C for later analysis.

Body mass index (BMI = weight (kg) / height (m<sup>2</sup>)) was then calculated. The levels of human serum testosterone (T), estradiol (E2) and progesterone (P4), follicle-stimulating hormone (FSH) and luteinizing hormone (LH) were measured by chemiluminescence assays (Diagnostic Products Corporation, Los Angeles, CA, USA). The concentrations of human serum total cholesterol (TC), HDL-cholesterol (HDL-C), LDL-C and TG were measured by enzymatic assay (Siemens Healthcare Diagnostics Inc., Tarrytown, NY, USA). Human serum PCSK9 concentrations were measured with an ELISA (R&D Systems; DPC900) according to the manufacturer's instructions. The intra- and interassay coefficients of variation for all measurements were <5 and 10%, respectively.

### 2.3. Animal Experiment

PCOS model mice were produced according to Lai *et al.* [20]. Female C57BL/6J mice, 21 days of age, were purchased from Chengdu Dashuo Biological Technology (SCXK (chuan) 2015-030). All animals were kept in standard environmental conditions (20 °C, 12 h light per day) with free access to rodent feed and water according to the institutional guidelines. At postnatal day 25, the mice were randomly divided into four groups ( $n = 40$  per group): the control group mice fed a normal chow and injected (s.c.) daily with sesame oil (0.1 mL); the PCOS group mice induced by feeding HFD (60% of calories from fat; Research Diets) and injecting (s.c.) daily with DHEA (6 mg per 100 g body weight) dissolved in 0.1 mL of sesame oil in the neck once a day for 20 consecutive days; the PCOS plus alirocumab group, which was alirocumab dissolved in saline and injected (3 mg/kg body weight in 0.1 mL saline) once every 5 days, the dose of alirocumab administered was equivalent to that for the treatment of patients with hypercholesterolemia [21,22]; and the PCOS plus vehicle (saline treatment was used as control solution) group. During the entire period of treatment, the animals were weighed every 4 days, and vaginal smears were taken daily beginning 10 days after the first injection until the end of the experiments. The stage of estrous cycle was determined by microscopic analysis of the predominant cell type in vaginal smears. After 20 days of treatment, the mice in each group were assessed to determine whether the PCOS model mice were successfully established. To eliminate the effect of estrous cycle on other detecting indicators, only those mice that were sacrificed on the estrus stage were used. The blood of all mice collected after an overnight fasting was centrifuged, and serum samples were collected and stored in a freezer at –80 °C for various biochemical analyses and ELISA. The left ovary and part of the liver of each mouse were dissected for the measurement of lipid contents and histochemical staining with hematoxylin and eosin (H&E) and immunohistochemical analysis. RNA for qPCR and protein for western blot were extracted from the right ovary and remaining liver tissue.

### 2.4. Analysis of Serum Hormone Concentrations

Serum T, E2 and P4 concentrations of mice were measured using commercial Iodine [<sup>125</sup>I] Radioimmunoassay Kits (North Institute of

Biological Technology, Beijing, China). The intra- and inter-assay errors among all assays were <10% and 15%, respectively. The limits of sensitivity were 0.02 ng/mL for T, 5 pg/mL for E2 and 0.2 ng/mL for P4, and the intra- and interassay coefficients of variability (CV) among all assays were <10% and 15%, respectively.

Serum concentrations of FSH and LH were measured with appropriate ELISA kits (Elabscience Biotechnology Co., Ltd., Wuhan, China). The LH assay has a detection limit of 0.28 ng/mL and the intra- as well as interassay CVs were <10%. The FSH assay has a detection limit of 0.94 ng/mL, and intra- as well as interassay CVs were <10%.

### 2.5. Lipid Profiles Analysis

Serum samples of mice were analyzed with biochemical analysis kits (Nanjing Jiancheng Bioengineering Institute, Nanjing, China) to determine serum lipid profiles, including TC, HDL-C, LDL-C and TG.

### 2.6. Histological Staining

Paraffin-embedded tissues were sectioned at 4  $\mu$ m, stained with H&E according to standard histological procedures and examined under a light microscope by two histologists blinded to the origin of the section.

### 2.7. Oil Red O Staining

Frozen 10- $\mu$ m tissue sections were stained with Oil Red O to detect neutral lipid accumulation according to the standard procedure [23]. Briefly, the sections were fixed at room temperature in 4% ORO Fixative for 10 min, washed with distilled water, and rinsed in 60% isopropanol for 2 min and in Oil Red O solution (G1260, Solarbio, Beijing, China) for 10 min. The slides were then rinsed in distilled water for 5 min and counterstained with Mayer's hematoxylin before mounting with Glycerol Jelly Mounting Medium (G2150, Solarbio, Beijing, China). The tissue sections were observed under an Olympus microscope (Olympus, Tokyo, Japan), and photographs were taken.

### 2.8. Transmission Electron Microscopy (TEM)

Ovarian tissue samples were cut into 1-mm<sup>3</sup> sections and fixed in 2.5% glutaraldehyde (pH 7.4) for 4 h. The sample was flushed with 0.1 M phosphate buffer (pH 7.2) three times and fixed in osmic acid for 2 h. Then the block, after acetone dehydration, was embedded in Epon-Araldite resin (Ted Pella, 18,030). Semi-thin sections were cut into ultrathin sections and counterstained with 3% uranyl acetate and 0.3% lead citrate. Then the cells of ovarian tissue were observed with a JEM1230 transmission electron microscope (JEOL, Japan).

### 2.9. Immunohistochemistry (IHC)

IHC was performed according to the SP kit instructions (SP-9001, ZSGBIO, Beijing, China). Briefly, the paraffin sections were deparaffinized in two changes of xylene and then rehydrated in decreasing concentrations of ethanol. Sodium citrate (0.1 M, pH 6.0) was used to restore antibody activity in a microwave oven for 20 min. Endogenous peroxidase was inactivated by 3% hydrogen peroxide at room temperature for 10 min. After three washes in PBS, the tissue sections were blocked for 30 min at 37 °C. The primary antibodies against PCSK9 (1:100; 55206-1-AP; Proteintech, Wuhan, China), LDLR (1:500; ab52818; Abcam, Cambridge, MA, USA) were incubated with the sections overnight at 4 °C. The corresponding secondary antibodies were incubated with the sections for half an hour at 37 °C. The sections were washed five times in PBS for 5 min per time. The sections were incubated in horseradish enzyme-labelled chain avidin solution for 30 min at 37 °C and washed in PBS for 5 min for five times. DAB staining and hematoxylin counterstaining were performed. Photographs were taken using an Olympus microscope (Olympus, Tokyo, Japan). As a

negative control, duplicate sections were immunostained without exposure to primary antibodies, which were replaced with PBS.

### 2.10. Evaluation of Ovulatory Function

After 20 days of the treatments, the animals were superovulated by the intraperitoneal injection of 10 IU of pregnant mare's serum gonadotropin (PMSG; Chifeng Boen Pharmaceutical Company, Neimenggu, China) followed by 10 IU human chorionic gonadotropin (hCG; Livzon Pharmaceutical Group Company, Guangdong, China) 48 h later. Cumulus-oocyte complexes were collected 16 h after hCG injection by puncturing the oviductal ampulla with a fine pair of forceps and a syringe and needle under a stereomicroscope, and the cumulus cells were removed by brief incubation in 0.2% hyaluronidase. Denuded oocytes were observed under a stereomicroscope. Oocytes with a round clear zona pellucida, a small perivitelline space and a pale, moderately granular cytoplasm that is devoid of inclusions were considered to be 'normal' [24]. The total number of ovulated oocytes in each mouse was used as the ovulation rate.

### 2.11. Serum PCSK9 ELISA Assay

Serum PCSK9 concentrations of mice were measured by sandwich ELISA (R&D Systems; MPC900) according to the manufacturer's instructions. Each sample was measured in duplicates. The intra-assay CV was 5.4%, whereas the interassay CV was 7.1%.

### 2.12. Quantitative Real-Time PCR

Total RNA of liver and ovary tissue was isolated using TRIzol reagent (Invitrogen, Carlsbad, CA, USA) according to the manufacturer's instructions. Real-time PCR was performed using a RevertAid First Strand cDNA Synthesis Kit (Thermo, Carlsbad, CA, USA) and SYBR Green probes (Bio-Rad, Foster City, CA, USA) according to the manufacturers' protocols. The sequences of primers used for measuring mRNA expression levels are shown in Supplemental Table 1. All measurements were performed in triplicate.  $\beta$ -actin was used as a reference gene to normalize gene expression. The values for relative quantification were calculated using the  $2^{-\Delta\Delta Ct}$  method after the threshold cycle.

### 2.13. Western Blotting

Tissues were harvested with a total protein extraction kit (PE001, Sabbiotech, College Park, MD, USA), and protein concentrations were measured with Enhanced BCA Protein Assay Kit (Beyotime Company, Jiangsu, China). The extracts (50  $\mu$ g protein) were loaded into each lane. The primary antibodies used were anti-PCSK9 rabbit polyclonal antibody (1:500; 55206-1-AP, Proteintech, Wuhan, China), anti-LDLR rabbit polyclonal antibody (1:5000; ab52818; Abcam, Cambridge, MA, USA) and rabbit anti- $\beta$ -actin rabbit polyclonal antibody (1:1000; bs-0061R; Bioss, Beijing, China). The secondary antibody used was HRP-labelled goat anti-rabbit IgG (1:1000; bs-0295G-HRP; Bioss, Beijing, China). Chemiluminescence reagent (Amersham, Piscataway, NJ) was used to visualize the blots. All experiments were repeated at least three times. The band density was quantified using ImageJ software (<https://imagej.nih.gov/ij/>).

### 2.14. Cell Isolation and Culture

TICs and GCs were isolated from 21-day-old immature C57BL/6 female mice and cultured following published protocols with minor modifications [25]. Briefly, isolated ovaries were immediately transferred to pre-warmed Medium 199 (GIBCO, Grand Island, NY) containing 0.1% BSA, 100 IU/mL penicillin and 100  $\mu$ g/mL streptomycin. Ovaries were cleaned of any surrounding tissue and repeatedly punctured with a 25-gauge needle in a Falcon dish to release GCs. The remaining ovarian

tissues were reserved for TICs isolation. GCs suspensions were then centrifuged at 1000 rpm for 5 min and resuspended in DMEM/F12 medium containing 0.1% BSA, 10% FBS, 100 IU/mL penicillin and 100 µg/mL streptomycin. After washing three times, the GCs were transferred to the DMEM/F12 medium. After overnight incubation, the wells were washed with DMEM/F12 medium to remove unattached cells. Cellular morphology was observed under the microscope.

The residual ovarian tissue was washed three times with Medium 199 and incubated for 60 min at 37 °C in Medium 199 supplemented with 4 mg/mL collagenase I (Worthington Biochemical Corp, Lakewood, NJ), 10 µg/mL DNase I (Worthington Biochemical Corp, Lakewood, NJ) and 0.1% BSA. During this time, the ovarian tissue was agitated using a pipette at least 20 times at intervals of 15 min. The dispersed cells were then centrifuged at 1000 rpm for 5 min and washed three times with Medium 199. Isolated TICs and GCs were counted with a hemocytometer. The cell viability was determined with trypan blue staining. TICs and GCs were transferred to separate culture plates containing a known volume of Medium 199 supplemented with 0.1% BSA, 1% FBS, 1% insulin-transferrin-selenium (GIBCO, Grand Island, NY, USA), 100 IU/mL of penicillin and 100 µg/mL streptomycin or DMEM/F12 medium containing 0.1% BSA, 10% FBS, 100 IU/mL penicillin, and 100 µg/mL streptomycin, respectively. After overnight incubation, the wells were washed with basal medium to remove unattached cells. Cells were then cultured for 24 h with either basal medium alone or medium supplemented with recombinant mouse PCSK9 (CA86) and/or alirocumab at concentrations, as indicated below.

### 2.15. LDL Uptake Assay

The LDLR activity of the TICs and GCs was determined using the BODIPY™ FL LDL uptake kit (I34359, Thermo Fisher Scientific, USA) according to the manufacturer's instructions. Briefly, TICs and GCs were separately cultured in glass-bottom dishes 35 mm (NEST) with  $2.0 \times 10^6$  cells/well. Then, the cells were treated with 0 (control), recombinant mouse PCSK9 (CA86) 7000 ng/mL and recombinant mouse PCSK9 (CA86) 7000 ng/mL plus 8000 ng/mL alirocumab for 4 h, and the culture medium was removed and replaced with 6 µg/mL BODIPY™ FL LDL in serum-free culture medium. After incubation for 3 h at 37 °C, the culture medium was removed and replaced with fresh culture medium. The degree of LDL uptake was examined under a Zeiss LSM880 confocal microscope with filters capable of measuring excitation and emission wavelengths 540 and 570 nm.

### 2.16. Statistical Analysis

All statistical analyses were performed with the software Prism (GraphPad, San Diego, CA). The Student's *t*-test was used for normal or parametric variables to compare two groups, and ANOVA followed by Bonferroni post-test was used to compare three groups. Multivariate linear regression analysis was performed to evaluate serum PCSK9 changes in the human population adjusting for age and BMI. Correlation was calculated using Pearson's correlation coefficient. Data are presented as mean  $\pm$  SD.  $P < 0.05$  was considered statistically significant.

## 3. Results

### 3.1. Serum PCSK9 Level Increased in the Women with PCOS

The analysis of clinical and biochemical profiles in women with PCOS and age-matched normal controls is shown in Supplemental Table 2. Higher values for BMI, T, LH, FSH, TC, TG, and LDL-C were found for patients with PCOS than those in control group ( $P < 0.05$ ). Moreover, the result of the ELISA assay showed that the serum PCSK9 level was significantly higher in the women with PCOS than it was in the controls ( $P = 0.0289$ ; Fig. 1). After adjusting for age and BMI, the differences in serum PCSK9 concentrations between the two groups

remained statistically significant ( $P < 0.05$ ). The relationships between serum PCSK9 levels and the serum lipid profiles and hormone concentrations were also analyzed, and the results indicated that serum PCSK9 was positively correlated with T ( $r = 0.207$ ,  $P = 0.044$ ), but not with LDL-C, TC, TG, HDL-C, E2, P, LH and FSH in two groups.

### 3.2. The Expression of PCSK9 Increased in the Serum, Livers and Ovaries of PCOS Mice

The PCOS model was successfully established in the mice including irregular estrous cycles, increased atretic and cystic follicles, decreased corpus luteum (CL), and increased serum T level (Fig. S1). As shown in Fig. 2A, serum PCSK9 levels in the PCOS mice were significantly higher than controls ( $P < 0.05$ ; Fig. 2A). Correspondingly, serum PCSK9 concentrations were significantly reduced in PCOS mice treated by alirocumab compared with those treated with vehicle ( $P < 0.05$ ; Fig. 2A).

Immunohistochemical staining showed that PCSK9 was mainly expressed in the hepatocytes and CL, ovarian medulla, GCs, TICs and oocytes, with higher levels in PCOS mice compared with the controls, which could be reversed by alirocumab administration (Fig. 2B, G). qPCR and western blot were used to examine PCSK9 expression in the mouse hepatic and ovarian tissues, and the results indicated that PCSK9 mRNA and protein levels in the livers and ovaries were increased in the PCOS mice, compared with the control mice ( $P < 0.05$ ; Fig. 2). As expected, the PCSK9 protein level of both livers and ovaries in the PCOS mice was reduced by alirocumab, an inhibitor of PCSK9; it nearly reached a similar level to that of the controls ( $P < 0.05$ ; Fig. 2).

### 3.3. PCSK9 Involved in Lipid Metabolic Disorders in PCOS Mice

To investigate whether PCSK9 is involved in lipid metabolic disorders of PCOS, body weight and the serum lipid profile (TC, LDL-C, HDL-C and TG) of the mice were determined. Body weight of the mice was similar before the treatments. From Days 4 to 20 of the treatments, the PCOS, PCOS plus alirocumab and PCOS plus vehicle mice exhibited significantly more weight gain than control mice ( $P < 0.05$ ; Fig. S2). In addition, the PCOS mice exhibited significantly higher serum TC, LDL-C and HDL-C levels than control mice ( $P < 0.05$ ; Fig. 3A-D). However, no difference of serum TG was found in the PCOS mice compared with controls (Fig. 3B). We further investigated the correlation between PCSK9 and metabolic parameters in the control and PCOS mice. As shown in Fig. 3, serum PCSK9 was positively correlated with LDL-C ( $r = 0.5279$ ,  $P = 0.0004$ ) and TC ( $r = 0.4151$ ,  $P = 0.0350$ ) but not with serum TG or HDL-C. Interestingly, when PCOS mice were simultaneously administered alirocumab, TC and LDL-C levels were significantly decreased compared with the PCOS mice that received the vehicle ( $P < 0.05$ ; Fig. 3).

Liver morphology was similar among the mice, as shown by H&E staining (Fig. 3I). However, compared with the controls, there was a

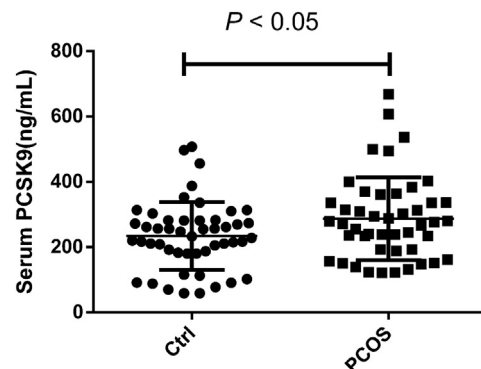
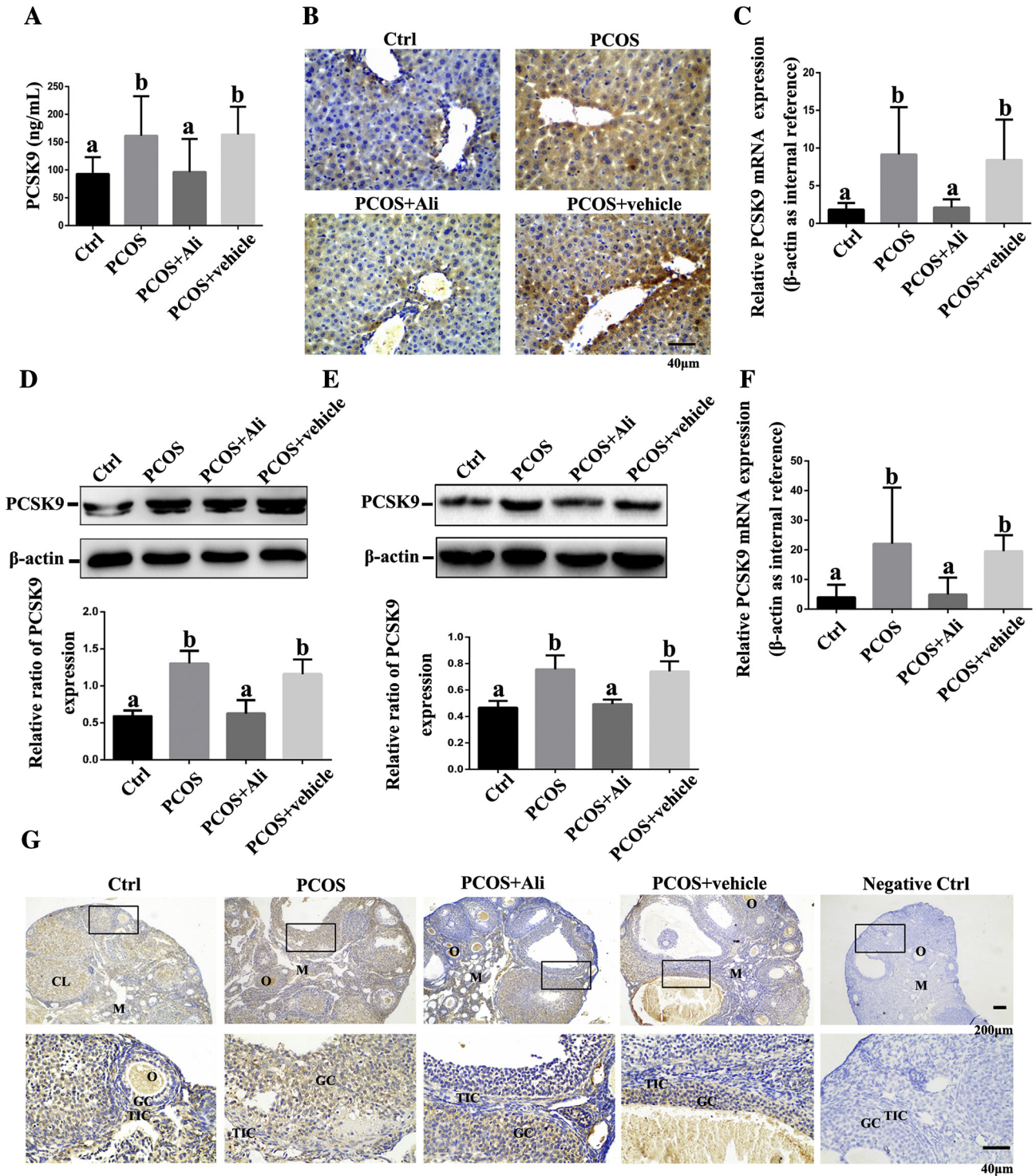


Fig. 1. Serum PCSK9 levels increased in the PCOS women. Data are presented as mean  $\pm$  SD;  $P < 0.05$  indicates statistical significance.

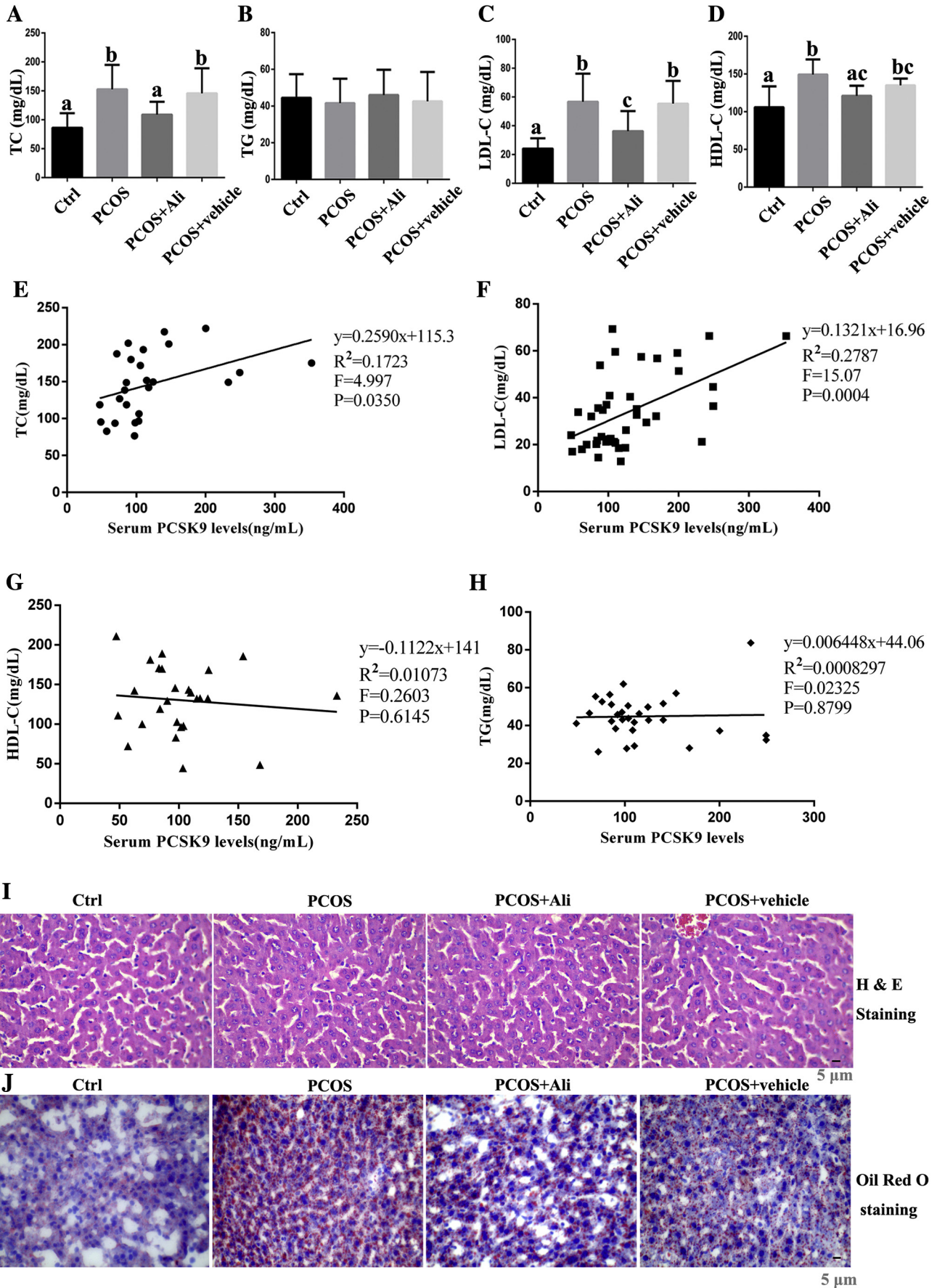


**Fig. 2.** The expression of PCSK9 in the blood, liver and ovary of the mice of the four groups. (A) Serum PCSK9 levels by the ELISA assay.  $n = 21$  per group. (B) Immunohistochemical staining of livers in the mice of different groups. Brown staining represents the positive expression of PCSK9, bar = 40  $\mu\text{m}$ . (C) The expression of PCSK9 mRNA in the liver by real-time PCR analysis. (D) Western blot analysis and densitometry quantification of PCSK9 protein in the liver. (E) Western blot analysis and densitometry quantification of PCSK9 protein in the ovary. (F) Real-time PCR analysis of the gene expression of PCSK9 mRNA in the ovary. (G) Immunohistochemical staining from representative ovarian section of mice, bar = 200  $\mu\text{m}$ , 40  $\mu\text{m}$ . GC, granulosa cell; TIC, theca-interstitial cell; CL, corpus luteum; M, ovarian medulla; O, oocyte. Data are presented as mean  $\pm$  SD; different lower-case letters above the columns, such as a and b, indicate  $P < 0.05$ , and if 2 columns have the same lowercase letter, it indicates no statistical significance.  $n = 5$  per group.

dramatic increase in hepatic lipid accumulation in PCOS mice, which could be reversed by alicumab administration, as revealed by Oil Red O staining (Fig. 3J).

To explore the mechanism of PCSK9's effect on the lipid metabolism in PCOS mice, LDLR mRNA and protein's expression in the mouse liver

were determined. The results indicated that LDLR mRNA was slightly decreased in the livers of PCOS mice, compared with those of the control mice, although it was not significantly different (Fig. 4B). Immunohistochemistry showed that LDLR was mainly located in the hepatocytes, with lower level in the liver of PCOS mice (Fig. 4A). Western blot also



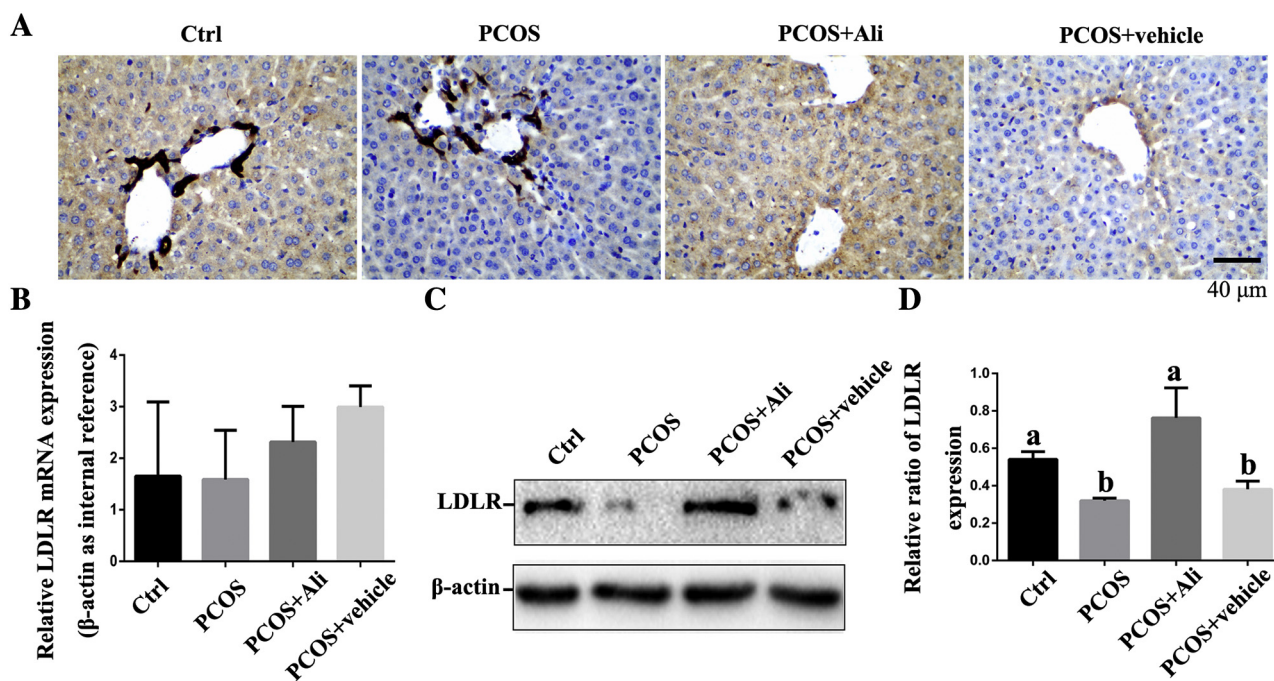


**Fig. 4.** The expression of LDLR of livers in the mice with different treatments. (A) Immunohistochemical sections from representative livers of mice. Brown staining represents the positive expression of LDLR. Bar = 40  $\mu$ m. (B) Gene expression of LDLR in the livers by real-time PCR analysis. (C, D) Western blot analysis and densitometry quantification of LDLR in the livers. Data are presented as mean  $\pm$  SD; different lower-case letters above the columns, such as a and b, indicate  $P < 0.05$ , and if 2 columns have the same lowercase letter, it indicates no statistical significance.  $n = 5$  per group.

demonstrated a lower level of LDLR in the liver from PCOS mice in comparison with the liver from the control mice ( $P < 0.05$ ; Fig. 4C, D), and inhibition of PCSK9 by alirocumab could cause upregulation of LDLR ( $P < 0.05$ ; Fig. 4).

#### 3.4. PCSK9 Directly Affects Ovarian Lipid Metabolism in PCOS Mice

Weight of the right ovaries did not differ among the four groups of mice (Fig. S2). Oil red O staining was primarily localized in the ovarian GCs, theca cells, CL and interstitial tissues of the mice, and there were visibly higher levels of lipids in the ovaries of PCOS mice versus the controls, whereas alirocumab treatment completely reversed the lipid augmentation in PCOS mice (Fig. 5A). TEM showed that there were many more lipid droplets in ovarian cells in the PCOS mice, and inhibition of PCSK9 can decrease the accumulated lipid droplets in the cells (Fig. 5B).

Correspondingly, immunohistochemistry indicated that besides some staining for LDLR in the GCs and TICs, the staining was mainly located in the CL and ovarian medulla, with lower levels in the ovaries of PCOS mice (Fig. 5C). qPCR and western blot both demonstrated a lower level of LDLR expression in the ovaries from PCOS mice in comparison with that from the controls, and it could be upregulated by alirocumab supplementation (Fig. 5D-F;  $P < 0.05$ ).

An *in vitro* LDL uptake showed that LDL uptake of mouse TICs and GCs was decreased by exogenous recombinant PCSK9, which could be reversed by alirocumab, as significant differences in relative fluorescence intensity indicating LDL uptake were found among control, recombinant mouse PCSK9-treated and recombinant mouse PCSK9 plus alirocumab-treated cells (Fig. 6).

#### 3.5. Inhibiting PCSK9 Partly Reverses Ovarian Function Disorders in PCOS Mice

The examination of hormones showed that the serum T, E2, and LH concentrations were significantly higher in combination with an increased LH/FSH ratio in the PCOS group than in the controls ( $P < 0.05$ ; Fig. 7B, C). Moreover, there was a significant decrease in T, E2, LH and the LH/FSH ratio in PCOS plus alirocumab group compared with the PCOS plus vehicle mice ( $P < 0.05$ ; Fig. 7). No difference in serum P4 and FSH concentrations was observed among the four groups of mice (Fig. 7).

As shown in Fig. S1, the PCOS mice exhibited the typical change of ovarian morphology, whereas the ovaries of PCOS mice treated with alirocumab exhibited follicles rescued in different stages of development, and no ovarian cysts were found. However, the ovaries of the PCOS mice treated with vehicle still had multiple cystic follicles (Fig. 7J).

To investigate ovulatory function of the mice, they underwent induced superovulation with PMSG and hCG. As shown in Fig. 7, the total number of ovulatory oocytes per PCOS mouse significantly increased, but many mature oocytes exhibited abnormal morphology with enlarged perivitelline space, fragmented cytoplasm or giant polar bodies. Interestingly, alirocumab treatment was effective in restoring the total number of ovulatory oocytes and their morphology ( $P < 0.05$ ; Fig. 7).

## 4. Discussion

In the present study, we have obtained important findings as follows: firstly, serum PCSK9 concentrations were significantly higher in PCOS patients than normal controls. Furthermore, the expression of PCSK9 in serum, livers and ovaries of PCOS mice was increased and

**Fig. 3.** Serum metabolic profiles and liver lipid deposition in the mice with different treatments. (A) Serum TC levels. (B) Serum TG levels. (C) Serum LDL-C levels. (D) Serum HDL-C levels.  $n = 28$  mice per group. (E–H) Correlations of the serum levels of PCSK9 with (E) TC, (F) LDL-C, (G) HDL-C, and (H) TG in the serum from the control and PCOS mice. (I) Liver morphology by H&E staining among the mice of different groups.  $n = 8$  per group. (J) Lipid content by Oil Red O staining in the liver from the mice of different groups.  $n = 5$  per group. Bar = 5  $\mu$ m. Data are presented as mean  $\pm$  SD; different lowercase letters above the columns, such as a, b, and c, indicate  $P < 0.05$ , and if 2 columns have the same lowercase letter, it indicates no statistical significance.

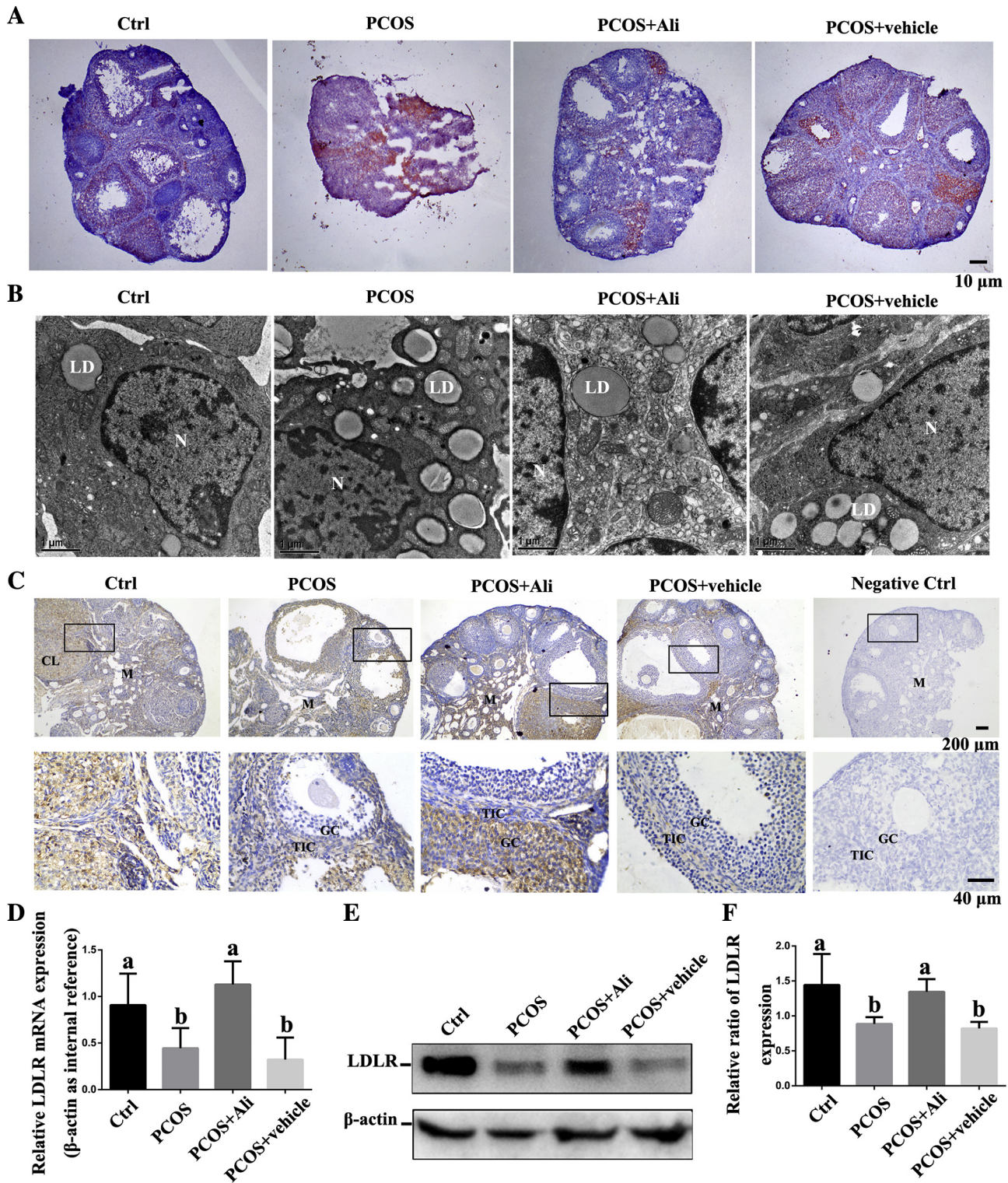


**Fig. 5.** The ovarian lipid deposition and the expression of LDLR in ovaries of the four groups. (A) Representative photomicrographs of ovary sections stained with Oil Red O in the mice. Bar = 10  $\mu$ m. (B) Represents electron micrographs as control, PCOS, PCOS plus alirocumab, and PCOS plus vehicle, taken with a TEM. N, nucleus; LD, lipid droplets. Bar = 1  $\mu$ m. (C) Immunohistochemical sections from representative ovaries of mice. Brown staining represents the positive expression of LDLR, bar = 200  $\mu$ m, 40  $\mu$ m. GC, granulosa cell; TIC, theca-interstitial cell; CL, corpus luteum; M, ovarian medulla. (D) Gene expression of LDLR in the ovaries by real-time PCR analysis. (E, F) Western blot analysis and densitometry quantification of LDLR in the ovaries. Data are presented as mean  $\pm$  SD; different lower-case letters above the columns, such as a and b, indicate  $P < 0.05$ , and if 2 columns have the same lowercase letter, it indicates no statistical significance.  $n = 5$  per group.

this marker positively correlated with TC and LDL-C. Finally, PCSK9 directly affected ovarian lipid metabolism and ovarian function in PCOS mice; the inhibition of PCSK9 with alirocumab partly improved the disrupted lipid profiles and the morphologic and functional ovarian

abnormality including endocrine, follicular growth and ovulation disorders in PCOS mice.

Dyslipidemia, the most prevalent metabolic aberration in PCOS, is often characterized by elevated TC and LDL-C, which are critically

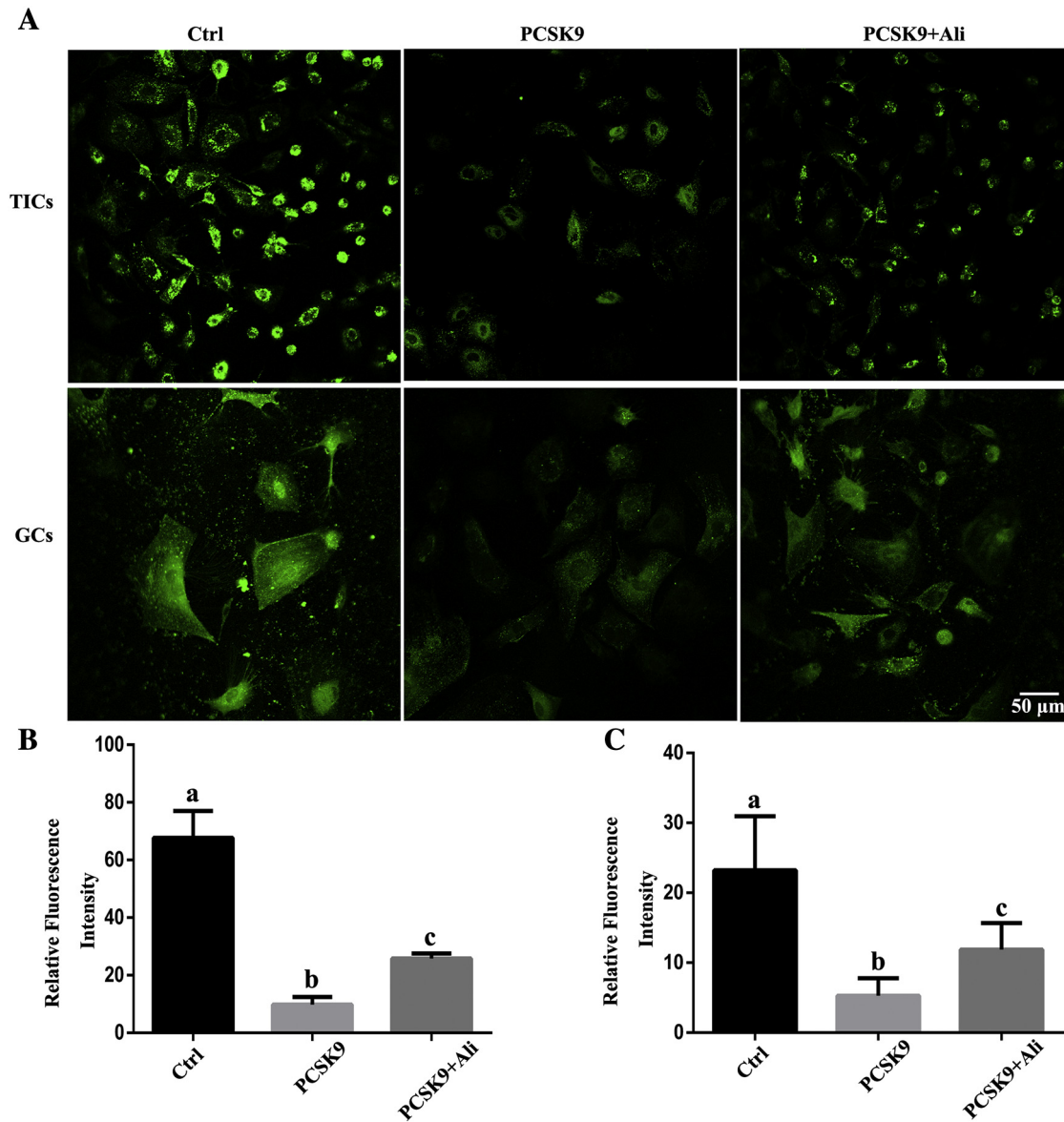


**Fig. 6.** The effect of recombinant mouse PCSK9 and PCSK9 plus alirocumab on PCSK9-mediated reduction of LDL uptake in TICs and GCs. (A) Representative LDL uptake assay of TICs and GCs from each group, bar = 50  $\mu$ m. (B) The degree of LDL uptake in TICs disposed with recombinant mouse PCSK9 (7000 ng/mL) or PCSK9 plus alirocumab (8000 ng/mL) for 4 h. (C) The degree of LDL uptake in GCs disposed with recombinant mouse PCSK9 or PCSK9 plus alirocumab for 4 h. Values were represented as mean  $\pm$  SD of three independent experiments; different lower-case letters above the columns, such as a and b, indicate  $P < 0.05$ , and if 2 columns have the same lowercase letter, it indicates no statistical significance.

involved in reproductive and metabolic complications of the syndrome [4,26]. In this research, we studied the role of PCSK9, a negative regulator of LDL-C, in the pathogenesis of PCOS. The result of our case-control study in 46 PCOS patients and 49 control women showed that serum PCSK9 levels are obviously increased in PCOS patients. This is the first important evidence of PCSK9 being involved in PCOS. However, Xavier et al. [27] found that plasma PCSK9 levels did not differ between PCOS patients and healthy women in Brazil. The contrary finding may be due to the differences in populations and PCSK9 genetic polymorphisms. We further analyzed the correlation between PCSK9 levels and the serum lipid profiles and hormone concentrations, and found that serum PCSK9 was positively correlated with testosterone, but not with LDL-C, TC, TG, HDL-C, E2, P, LH and FSH when women with PCOS and normal women were analyzed together, which was inconsistent with our predictions. We analyze the major reason is the limited number of clinical samples.

To validate the results of the case-control study that PCSK9 is involved in PCOS, we used female C57 BL/6J mice to successfully establish

PCOS model animals with the basic characteristics of PCOS including irregular estrous cycles remaining in constant estrus (suggesting anovulation), impaired ovarian morphology (showing multiple large cysts with diminished granulosa layers and increased thecal layers and stromal-interstitial tissue in the ovarian tissues) and a marked increase in serum T levels. The important insight was that, as we expected, the high expression of PCSK9 in the serum and liver of the model mice, which was the accompaniment of dyslipidemia including high levels of circulating LDL-C and TC, and serum PCSK9 level was positively correlated with TC and LDL-C. PCSK9 overexpression in blood or liver results in hyperlipidemia, hypercholesterolemia, atherosclerosis, and CVD [28]. We also found that PCOS mice have increased hepatic lipid content compared with controls by Oil Red O staining. These results indicate a possible association of PCSK9 with the pathogenesis of PCOS.

PCSK9, as a lipid metabolic negative regulator, regulates cholesterol homeostasis exclusively via enhancing LDLR degradation, resulting in LDL accumulation in plasma [29,30]. We found that LDLR was present in the cytoplasm of hepatocytes from all the mice, but LDLR protein

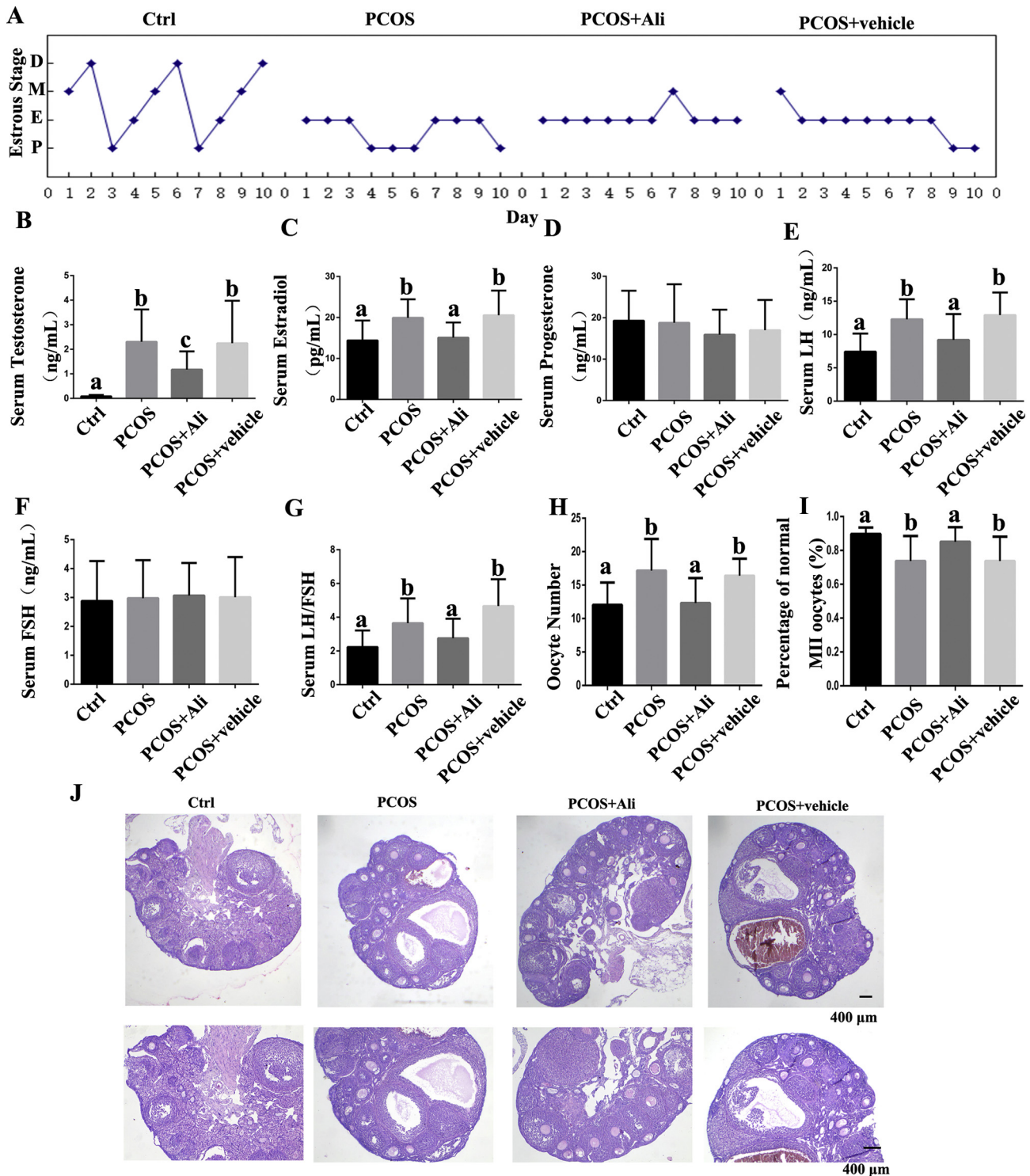


**Fig. 7.** Estrous cyclicity, hormone concentrations, ovarian morphology, and assessment of ovulatory capacity including the quantity and quality of oocytes in the mice of the four groups. (A) Representative estrous cycle of one mouse from each group. D, diestrus; M, metestrus; E, estrus; P, proestrus. (B) Testosterone, (C) estradiol, (D) progesterone, (E) LH, (F) FSH, (G) LH/FSH, (H) The number of oocytes, (I) The percentages of normal MII oocytes from each group. (J) Representative H&E staining of ovarian sections of mice from each group, bar = 400 μm. Data are presented as mean ± SD; different lower-case letters above the columns, such as a, b and c, indicate  $P < 0.05$ , and if 2 columns have the same lowercase letter, it indicates no statistical significance.  $n = 21$  per group.

level in the livers of PCOS mouse model was significantly lower, whereas PCSK9 levels were higher than that in the controls. The consistency of our above findings with other dyslipidemia populations [31] suggests that the PCOS may have an add-on effect of boosting circulating and hepatic PCSK9 expression and then increasing LDL-C levels—one possible mechanism responsible for the dyslipidemia of PCOS.

This has been further proved through the administration of alirocumab, a PCSK9 monoclonal antibody (also known as SAR236553/REGN727), which consistently reduced circulating TC and LDL-C and decreased the redundant hepatic and ovarian lipid content in PCOS mice. PCSK9 inhibition attenuates progression of lipid dysfunction of various organs and tissues [28] and decreases LDL-C levels and CVD risk [32]. Moreover,

the treatment with alirocumab significantly decreased the liver PCSK9 protein level and increased the LDLR protein level. Previous studies have shown that PCSK9 is presently considered as a likely safe target for cholesterol-lowering therapy [33,34], and alirocumab may bind circulating PCSK9 and block its interactions with surface LDLR to treat hypercholesterolemia for LDL-C reduction [35,36]. It seems obvious that PCSK9 is involved in the lipid metabolic disorders of PCOS.

Another important characteristic of PCOS is ovarian dysfunction including endocrine, follicular growth and ovulation disorders. We have every reason to believe that dyslipidemia induced by PCSK9 leads to abnormal functions in PCOS model mice. As we know, cholesterol is essential for ovary functions, as it is the precursor for all steroid hormones and material for follicular growth [16]. Recent studies have indicated when there is dyslipidemia in the body, a large amount of androgen is produced under the action of 17 $\alpha$ -hydroxylase and 17,20-lyase; then androgen is transformed into estradiol, secreted by the follicles continuing to act on the hypothalamus and hypophysis, promoting the secretion of LH, producing high LH levels, which causes the follicle to develop abnormally. Without mature follicles, the immature follicles gradually become cystic or degenerate, eventually causing ovarian polycystic changes [17,37]. In the present study, we found disturbed lipid metabolism in addition; the PCOS mice also exhibited significantly increased estrus length, T and estradiol levels, elevated LH levels and LH/FSH ratio, and restrained ovarian follicular development, increased follicle atresia and cystic follicles—all consistent with the characteristics of the PCOS patients. In addition, the PCOS mice yielded more oocytes when they underwent a superovulatory regimen of PMSG plus hCG; however, there were fewer normal mature oocytes, indicating the poor quality of oocytes from PCOS mice. Furthermore, we found that alirocumab administration did not improve estrous cyclicity; however, T, E2, LH and LH/FSH ratio levels were significantly decreased, suggesting that alirocumab treatment could not only rescue lipid metabolism but also partly reverse levels of reproductive hormones of PCOS mice. Furthermore, although the PCOS mice treated with alirocumab ovulated fewer oocytes, the quality of oocytes was improved. The exact mechanisms by which PCSK9 alters oocyte competence are not completely understood in the PCOS mice, but abnormal lipid metabolism caused by PCSK9 appears to play an important role.

On the other hand, the PCSK9 expressed locally in the medulla, GCs, TICs, oocytes and CL of the ovaries possibly directly affects ovarian functions in PCOS model mice. The present study showed the overexpressing PCSK9 mRNA and protein in the ovary of PCOS mice, whereas the LDLR mRNA and protein were significantly decreased, indicating that PCSK9 may also inhibit the expression of LDLR in the mouse ovarian cells, so that their uptake of cholesterol must be influenced. Previous research showed that deletion of LDLR in theca cells can lead to lower estrogen biosynthesis and secretion [38]. Guo et al. [39] discovered that lack of LDLR results in dyslipidemia and poor fertility. In our *in vitro* experiment, LDL uptake capacity of both TICs and GCs exhibited a declining tendency when treated with recombinant mouse PCSK9; however, this effect can be reversed by simultaneously administering alirocumab, which is consistent with the LDL uptake in HepG2 cells [40]. Obviously, the decrease of LDL uptake (that is, decreasing cholesterol uptake) can affect the proliferation of follicle cells and their steroid hormone synthesis.

One limitation of this study is the small clinical sample size. Despite this, integrating clinical study and animal experiments is a strength of this study. Intervention experiments were also conducted in animals to further explain the involvement of PCSK9 in the pathogenesis of PCOS. This would provide new clue for future studies. In addition, the PCOS mouse model was induced by feeding HFD and injecting DHEA in our research and thus it should be confirmed both factors may have an impact on subsequent results; however, we have not yet determined which one plays a leading role in the expression of PCSK9. Further investigations are required to study the causes of abnormally high expression of PCSK9 in this PCOS mouse model, and deeply explore the mechanisms of PCSK9 in PCOS.

Above all, these data indicate that the increased PCSK9 in the PCOS mice may affect ovarian cholesterol metabolism and have an impact on the microenvironment for the development of follicles and steroid hormone synthesis by means of degradation of LDLR by PCSK9 to disrupt the uptake of cholesterol, whereas the decreased levels of PCSK9 and enhancement of LDLR with alirocumab treatment can partly reverse the impairment and ameliorate hyperlipidemia, as well as rescue ovarian functions. Thus, we conclude that PCSK9 overexpression in the blood, hepatic and ovarian tissue of PCOS mice might be involved in the development and progression of PCOS and that elevated levels of PCSK9 could be an early biomarker for PCOS; PCSK9 could be a therapeutic targeting molecule for PCOS.

Supplementary data to this article can be found online at <https://doi.org/10.1016/j.metabol.2019.02.002>.

## Author Contributions

MW participated in the study design, method investigation, experiment performance and the preparation of the manuscript; DZ and LX participated in clinical samples collection and data analysis; WG, LN, YL, YL, M L, YW, XZ, LZ, HL, and J Z performed the animal experiments; MW, YL, and YW carried out the qPCR analysis; MW and WG performed western blot analysis; and DY and LY were involved in the study design and the revision of the manuscript. All the authors approved the final version of the manuscript.

## Acknowledgements/Funding

The work was supported with grants from the National Natural Science Foundation of China (81771542, 81300535), the Sichuan Natural Science Foundation, China (2017JY0021) and the Fundamental Research Funds for the Central Universities (2012017jyjs189).

## Conflict of Interest

None.

## References

- [1] Conway G, Dewailly D, Diamanti-Kandarakis E, Escobar-Morreale HF, Franks S, Gambineri A, et al. The polycystic ovary syndrome: a position statement from the European Society of Endocrinology. *Eur J Endocrinol* 2014;171:P1–29.
- [2] Rotterdam EA-SPcwg. Revised 2003 consensus on diagnostic criteria and long-term health risks related to polycystic ovary syndrome (PCOS). *Hum Reprod* 2004;19:41–7.
- [3] Ferri N, Ruscica M. Proprotein convertase subtilisin/kexin type 9 (PCSK9) and metabolic syndrome: insights on insulin resistance, inflammation, and atherogenic dyslipidemia. *Endocrine* 2016;54:588–601.
- [4] Legro RS, Kunesman AR, Dunaif A. Prevalence and predictors of dyslipidemia in women with polycystic ovary syndrome. *Am J Med* 2001;111:607–13.
- [5] Rocha MP, Marcondes JA, Barcellos CR, Hayashida SA, Curi DD, Da Fonseca AM, et al. Dyslipidemia in women with polycystic ovary syndrome: incidence, pattern and predictors. *Gynecol Endocrinol* 2011;27:814–9.
- [6] Carmina E, Legro RS, Stamets K, Lowell J, Lobo RA. Difference in body weight between American and Italian women with polycystic ovary syndrome: influence of the diet. *Hum Reprod* 2003;18:2289–93.
- [7] Zhang F, Liu H. The dyslipidemia in women with polycystic ovary syndrome. *J Int Reprod Health Fam Plan* 2011;30:126–8.
- [8] Berneis K, Rizzo M, Lazzarini V, Fruzzetti F, Carmina E. Atherogenic lipoprotein phenotype and low-density lipoproteins size and subclasses in women with polycystic ovary syndrome. *J Clin Endocrinol Metab* 2007;92:186–9.
- [9] Vine DF, Wang Y, Jetha MM, Ball GD, Proctor SD. Impaired ApoB-lipoprotein and triglyceride metabolism in obese adolescents with polycystic ovary syndrome. *J Clin Endocrinol Metab* 2017;102:970–82.
- [10] Seidah NG, Benjannet S, Wickham L, Marcinkiewicz J, Jasmin SB, Stifani S, et al. The secretory proprotein convertase neural apoptosis-regulated convertase 1 (NARC-1): liver regeneration and neuronal differentiation. *Proc Natl Acad Sci U S A* 2003;100:928–33.
- [11] Tavori H, Rashid S, Fazio S. On the function and homeostasis of PCSK9: reciprocal interaction with LDLR and additional lipid effects. *Atherosclerosis* 2015;238:264–70.
- [12] Seidah NG, Awan Z, Chretien M, Mbikay M. PCSK9: a key modulator of cardiovascular health. *Circ Res* 2014;114:1022–36.
- [13] Abifadel M, Rabes JP, Devillers M, Munnich A, Erlich D, Junien C, et al. Mutations and polymorphisms in the proprotein convertase subtilisin kexin 9 (PCSK9) gene in cholesterol metabolism and disease. *Hum Mutat* 2009;30:520–9.

- [14] Rodgers RJ, Irving-Rodgers HF. Formation of the ovarian follicular antrum and follicular fluid. *Biol Reprod* 2010;82:1021–9.
- [15] Stouffer RL, Xu F, Duffy DM. Molecular control of ovulation and luteinization in the primate follicle. *Front Biosci* 2007;12:297–307.
- [16] Azhar S, Leers-Sucheta S, Reaven E. Cholesterol uptake in adrenal and gonadal tissues: the SR-BI and 'selective' pathway connection. *Front Biosci* 2003;8:s998–1029.
- [17] van Montfoort AP, Plosch T, Hoek A, Tietge UJ. Impact of maternal cholesterol metabolism on ovarian follicle development and fertility. *J Reprod Immunol* 2014;104–105:32–6.
- [18] Fujimoto VY, Kane JP, Ishida BY, Bloom MS, Browne RW. High-density lipoprotein metabolism and the human embryo. *Hum Reprod Update* 2010;16:20–38.
- [19] Rigotti A, Miettinen HE, Krieger M. The role of the high-density lipoprotein receptor SR-BI in the lipid metabolism of endocrine and other tissues. *Endocr Rev* 2003;24:357–87.
- [20] Lai H, Jia X, Yu Q, Zhang C, Qiao J, Guan Y, et al. High-fat diet induces significant metabolic disorders in a mouse model of polycystic ovary syndrome. *Biol Reprod* 2014;91:127.
- [21] Gaudet D, Kereiakes DJ, McKenney JM, Roth EM, Hanotin C, Gipe D, et al. Effect of alirocumab, a monoclonal proprotein convertase subtilisin/kexin 9 antibody, on lipoprotein(a) concentrations (a pooled analysis of 150 mg every two weeks dosing from phase 2 trials). *Am J Cardiol* 2014;114:711–5.
- [22] Kastelein JJ, Hovingh GK, Langslet G, Baccara-Dinet MT, Gipe DA, Chaudhari U, et al. Efficacy and safety of the proprotein convertase subtilisin/kexin type 9 monoclonal antibody alirocumab vs placebo in patients with heterozygous familial hypercholesterolemia. *J Clin Lipidol* 2017;11:195–203 [e4].
- [23] Trigatti B, Rayburn H, Vinals M, Braun A, Miettinen H, Penman M, et al. Influence of the high density lipoprotein receptor SR-BI on reproductive and cardiovascular pathophysiology. *Proc Natl Acad Sci U S A* 1999;96:9322–7.
- [24] Ubaldi F, Rienzi L. Morphological selection of gametes. *Placenta* 2008;29(Suppl. B):115–20.
- [25] Liu X, Qiao P, Jiang A, Jiang J, Han H, Wang L, et al. Paracrine regulation of steroidogenesis in theca cells by granulosa cells derived from mouse preantral follicles. *Biomed Res Int* 2015;2015:925691.
- [26] Chang AY, Oshiro J, Ayers C, Auchus RJ. Influence of race/ethnicity on cardiovascular risk factors in polycystic ovary syndrome, the Dallas Heart Study. *Clin Endocrinol (Oxf)* 2016;85:92–9.
- [27] Xavier LB, Soter MO, Sales MF, Oliveira DK, Reis HJ, Candido AL, et al. Evaluation of PCSK9 levels and its genetic polymorphisms in women with polycystic ovary syndrome. *Gene* 2018;644:129–36.
- [28] Kuhnast S, van der Hoorn JW, Pieterman EJ, van den Hoek AM, Sasiela WJ, Gusarova V, et al. Alirocumab inhibits atherosclerosis, improves the plaque morphology, and enhances the effects of a statin. *J Lipid Res* 2014;55:2103–12.
- [29] Dietschy JM, Turley SD, Spady DK. Role of liver in the maintenance of cholesterol and low density lipoprotein homeostasis in different animal species, including humans. *J Lipid Res* 1993;34:1637–59.
- [30] Zaid A, Roubtsova A, Essalmani R, Marcinkiewicz J, Chamberland A, Hamelin J, et al. Proprotein convertase subtilisin/kexin type 9 (PCSK9): hepatocyte-specific low-density lipoprotein receptor degradation and critical role in mouse liver regeneration. *Hepatology* 2008;48:646–54.
- [31] Zhang L, Song K, Zhu M, Shi J, Zhang H, Xu L, et al. Proprotein convertase subtilisin/kexin type 9 (PCSK9) in lipid metabolism, atherosclerosis and ischemic stroke. *Int J Neurosci* 2016;126:675–80.
- [32] Lambert G, Sjouke B, Choque B, Kastelein JJ, Hovingh GK. The PCSK9 decade. *J Lipid Res* 2012;53:2515–24.
- [33] Brown MS, Goldstein JL. Biomedicine. Lowering LDL—not only how low, but how long? *Science* 2006;311:1721–3.
- [34] Seidah NG, Prat A. The proprotein convertases are potential targets in the treatment of dyslipidemia. *J Mol Med (Berl)* 2007;85:685–96.
- [35] Pecin I, Reiner Z. Alirocumab: targeting PCSK9 to treat hypercholesterolemia. *Drugs Today (Barc)* 2015;51:681–7.
- [36] Tavori H, Melone M, Rashid S. Alirocumab: PCSK9 inhibitor for LDL cholesterol reduction. *Expert Rev Cardiovasc Ther* 2014;12:1137–44.
- [37] Robins ED, Nelson LM, Hoeg JM. Aberrant hypothalamic-pituitary-ovarian axis in the Watanabe heritable hyperlipidemic rabbit. *J Lipid Res* 1994;35:52–9.
- [38] McNatty KP, Makris A, DeGrazia C, Osathanondh R, Ryan KJ. The production of progesterone, androgens, and estrogens by granulosa cells, thecal tissue, and stromal tissue from human ovaries in vitro. *J Clin Endocrinol Metab* 1979;49:687–99.
- [39] Guo T, Zhang L, Cheng D, Liu T, An L, Li WP, et al. Low-density lipoprotein receptor affects the fertility of female mice. *Reprod Fertl Dev* 2015;27:1222–32.
- [40] Song KH, Kim YH, Im AR, Kim YH. Black raspberry extract enhances LDL uptake in HepG2 cells by suppressing PCSK9 expression to upregulate LDLR expression. *J Med Food* 2018;21:560–7.